Available online at www.derpharmachemica.com

Scholars Research Library

Der Pharma Chemica, 2015, 7(8):162-169
(http://derpharmachemica.com/archive.html)

ISSN 0975-413X
CODEN (USA): PCHHAX

Photovoltaic performance and influence of electrolyte on nano-titania based solar cells

Raman Kumar Saini†, Devender Singh†, Shri Bhagwan, Sonika, Ishwar Singh and Pratap Singh Kadyan*

Department of Chemistry, Maharshi Dayanand University, Rohtak, Haryana

---

ABSTRACT

The photovoltaic performance nano-titania based dye sensitized solar cells studied with different redox electrolytes containing inorganic (KI-I_2) and organic quaternary ammonium iodide salts i.e. $(CH_3)_4NI$-I_2, $(CH_3CH_2)_4NI$-I_2 and $(CH_3CH_2CH_2)_4NI$-I_2. Fabrications of solar devices were made using patent blue V dye on fluorine-doped tin oxide fused silica substrate. Titania (TiO_2) nanoparticles layer was applied as photo anode electrode and graphite layer was used as counter electrode. The electronic absorption spectra of dye was studied which showed peaks at 222 nm and 311 nm due to the $\pi \rightarrow \pi^*$ transitions of the aromatic rings of dye and peaks at 405 and 576 nm involved due to $n \rightarrow \pi^*$ transition of different aromatic rings available in dye molecule. The optical band gap of dyes was found 1.75 eV. Maximum V_{oc} (0.412 V) was found with $(CH_3CH_2)_4NI$-I_2 redox electrolyte. However maximum J_{sc} (0.219 mA/cm^2) was also obtained with maximum efficiency (0.476) with $(CH_3CH_2CH_2)_4NI$-I_2 redox electrolyte. Through the photovoltaic analysis the patent blue V dye was found suitable sensitizer for the fabrication of solar cell devices.

INTRODUCTION

Due to the global challenge for searching and developing of renewable energy sources, photovoltaic technologies become a topic of interest in the conversion of solar to electrical energy. The multijunction solar cell has been successfully performed in the laboratory scale up to 40% conversion efficiency [1]. However, their high production cost and toxicity to environment are still problems to use them as solar energy production[2]. Gratzel and O'Regan presented a photovoltaic device that is well-known as nanocrystalline dye-sensitized solar cell (DSSC). Since then, it has fascinated a lot of interest because of the conversion of solar energy to electricity [3-6]. Generally these cells composed of a wide band gap semiconductor deposited on a transparent conducting oxide (TCO) glass, molecular sensitizer and a redox electrolyte [7-9]. The most important parts of DSSC are mesoporous semiconductor oxide layers that composed of nanoparticles and monolayer of dye sensitizers that attached to the surface of the semiconductor nano-films [3]. The dye sensitizers play an important role in DSSC that have a significant influence on the photoelectric conversion efficiency and transport performance of electrode [10-12]. Up to now, over thousands of dye sensitizers were synthesized and tested, only several kinds of dye sensitizers have good performance in DSSC. In metal–organic complexes, especially the noble metal ruthenium polypyridyl complexes, including N3 and black dye etc. that were presented by Gratzel et al., have proved to be the best dye sensitizers with overall energy conversion efficiency greater than 10% under air mass (AM) 1.5 irradiation. In metal- free organic dyes sensitizers, including cyanines, hemicyanines, triphenylmethanes, perylenes, coumarins, porphyrins, squaraines, indoline, and azulene-based dyes etc., have also been developed because of their high molar absorption coefficient, relatively simple synthesis procedure, various structures and lower cost [13–14]. In contrast to the

numerous experimental studies of dye sensitizers, the theoretical investigations are relatively limited. Only several groups focused on the electronic structures and absorption properties of dye sensitizers [15–16] and organic dyes coupled TiO_2 nanocrystalline [17], as well as the electron transfer dynamics of the interface between dyes and nanocrystalline [18]. Until now, it remains a severe challenge for both experiment and theory to elucidate the fundamental properties of the ultrafast electron injection in DSSC and to approach the satisfied efficiency of DSSC. Further developments in dye design will play a crucial part in the ongoing optimization of DSSC [19], and it depends on the quantitative knowledge of dye sensitizer. So the theoretical investigations of the physical properties of dye sensitizers are very important in order to disclose the relationship among the performance, structures and the properties, it is also helpful to design and synthesis novel dye sensitizers with higher performance.

In present analysis the electronic, optical, thermal and photoelectrochemical properties of fabricated dye sensitized solar cells have been analyzed using organic patent blue V dye as sensitizer. The photovoltaic performance of fabricated DSSCs has been presented by using different electrolytes of quaternary alkyl ammonium iodide, KI/iodine (I_2) redox couple in acetonitrile solvent.

MATERIALS AND METHODS

Chemicals

Fluorine doped tin oxide (FTO) conducting glass with resistance 6-8 Ω/cm^2 was used as transparent substrate obtained from Sigma-Aldrich. The acetonitrile was employed as medium of electrolyte solution; potassium iodide (KI), iodine (I_2), tetramethylquaternaryammonium iodide [$(CH_3)_4NI$], tetraethylquaternaryammonium iodide [$(CH_3CH_2)_4NI$], tetrapropylquaternaryammonium iodide [$(CH_3CH_2CH_2)_4NI$] (Sigma–Aldrich) were purchased and used as without further purification. Titania P25 powder (nanocrystalline TiO_2) was used for preparing photoanode. Patent blue dye was also purchased from Sigma–Aldrich.

Instrumentation and measurements

The absorption spectra of the organic dyes were recorded by a Shimadzu 2450 spectrophotometer UV–Vis (range 180–1100 nm). Current–voltage curves were recorded by a digital Keithley 2450 Source meter connected to computer and controlled by kickstart software. Simulated light irradiation was used by a 200W tungsten (W) Arc lamp. Thermal gravimetric analysis (TGA) was performed on STA-7300 thermal analyzer of Hitachi. TGA and DTA curves were obtained by heating 35 to 500 ◦C at a heating rate of 10 ˚C/min in inert atmosphere.

Fabrication of Dye sensitized solar cell

Cleaning and masking of conducting substrate

Transparent substrate i.e. FTO coated conducting glass of adequate size were subjected to clean with cedepol neutral soap solution, then sonicated for 15 minutes, rinsed with distilled water several times. FTO coated conducting glass cleaned with reagent grade acetone were then sonicated in acetone for 15 minutes and then boiled in propan-2-ol solvent and finally dried under oven at 80 ^oC. The substrates were masked in order to deposit the thin film of composite material under consideration over the substrate. Plastic tape was used to cover the substrate in such a way that a small strip of etched portion was masked. This solved the purpose of exposing the bottom counter electrode for contact purpose during characterization of device.

Preparation of nanocrystalline TiO_2 layer

Titanium dioxide (P25) (1g) powder mixed with 1 ml of glacial acetic acid was put into the mortar and then further 0.25 ml increments of acid solution were added with the pipette while grinding with a pestle to get a uniform and lump free paste. The titanium dioxide paste in a small vial was sonicated for 30 minutes. The prepared TiO_2 paste was sprayed onto labeled FTO glass using doctor blade technique and then sintered at 300 ^oC for 2 h.

Preparation of dyes and electrolyte solutions

Patent blue V was dissolved in water to make a 0.1 M solution of dye. Titanium dioxide coated substrate was dipped in a dye solution for 24 h. Absorption of dyes on TiO_2 layer shown in figure 1. The electrolytes were prepared by mixing iodine (I_2) (0.01M) with potassium iodide (KI) (0.1M)/ tetramethylquaternaryammonium iodide [$(CH_3)_4NI$] (0.1M)/ tetraethylquaternaryammonium iodide [$(CH_3\ CH_2)_4NI$] (0.1M)/ tetrapropylquaternaryammonium iodide [$(CH_3CH_2CH_2)_4NI$] (0.1M) in acetonitrile solvent.

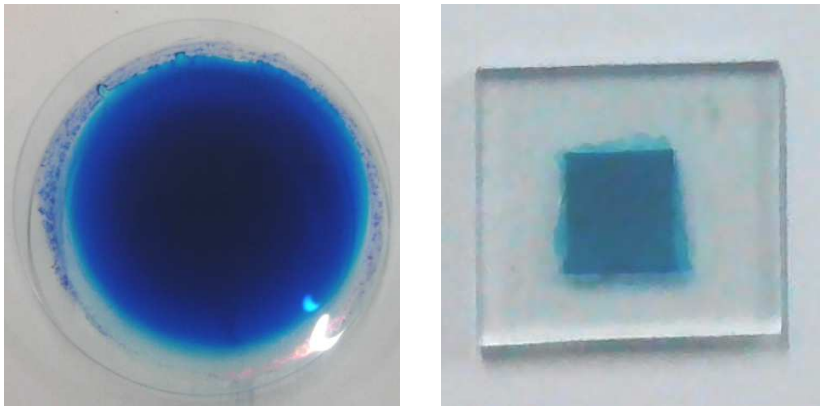

Figure 1. Schematic representation of patent blue V dye solution on watch glass and substrate coated with TiO_2 layer after dye absorption

RESULTS AND DISCUSSION

UV-Vis spectrum of patent blue V dye

The absorption spectra of patent blue V dyes in aqueous medium are shown in Fig. 2. The electronic absorption spectra of patent blue V dyes display four main bands. The energies corresponding to the absorption maximum presented in these spectra at wavelengths of 222 nm, 311 nm, 405 nm and 576 nm. The bands at 222 nm and 311 nm was assigned to the $\pi \rightarrow \pi^*$ transitions of the aromatic rings. The bands at 405 nm and 576 nm involves $n \rightarrow \pi^*$ transition which can be assigned to the non-bonding orbital of a lone pair on nitrogen atoms in the secondary amine group in the dye molecule. In many organic materials, it is usual to analyze the optical absorption at the fundamental edge in terms of band-to-band transitions theory. In this treatment, the absorption data follows a power-law behavior of Tauc [20] which is given by equ. (1):

$$\alpha=(A/h\nu)(h\nu-E_g)^m \qquad \text{----------equ. (1)}$$

where A is an energy-independent constant and E_g is the optical band gap. In order to determine a more precise value of the optical band gap, we plotted $(\alpha h\nu)^{1/2}$ as a function of photon energy. The optical band gap was determined by extrapolating the linear portion of the plot to $(\alpha h\nu)^{1/2} = 0$. This suggests that the fundamental absorption edge in the studied films is formed by the indirect allowed transitions. The calculated values of the optical band gap for patent blue V was 1.75 eV as shown in fig. 3. The indirect transition process is often included phonons. A phonon is either emitted or absorbed, depending on whether the energy of the photon is more than the indirect band gap or less. The density of these states falls off exponentially with energy which is consistent with the theory of Tauc [20]. It was found that the photon energy dependence of logarithm of absorption coefficient is expressed by the equation (2) :

$$\alpha= \alpha_o \exp(E/E_u) \qquad \text{----------equ. (2)}$$

where α_0 is a parameter dependent on photon energy and E_u is the Urbach energy and it can be evaluated as the width of the exponential absorption edge.

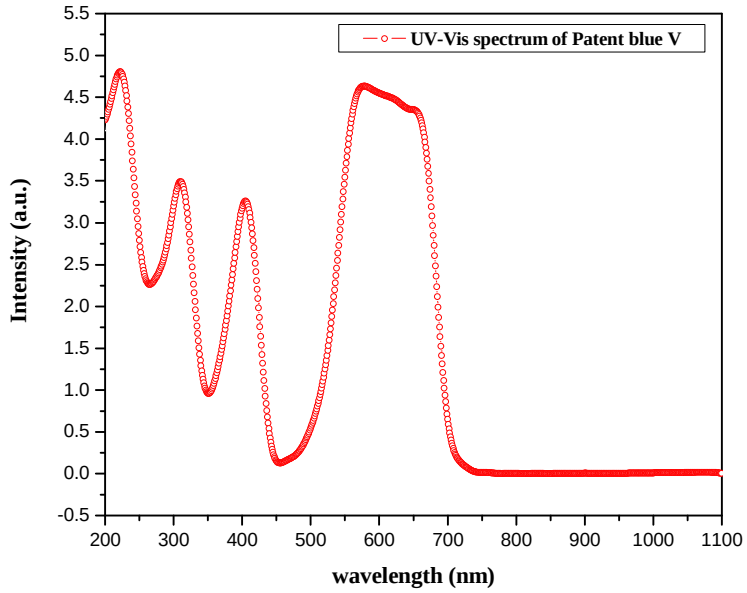

Figure 2. UV-Vis absorption spectrum of patent blue V dye

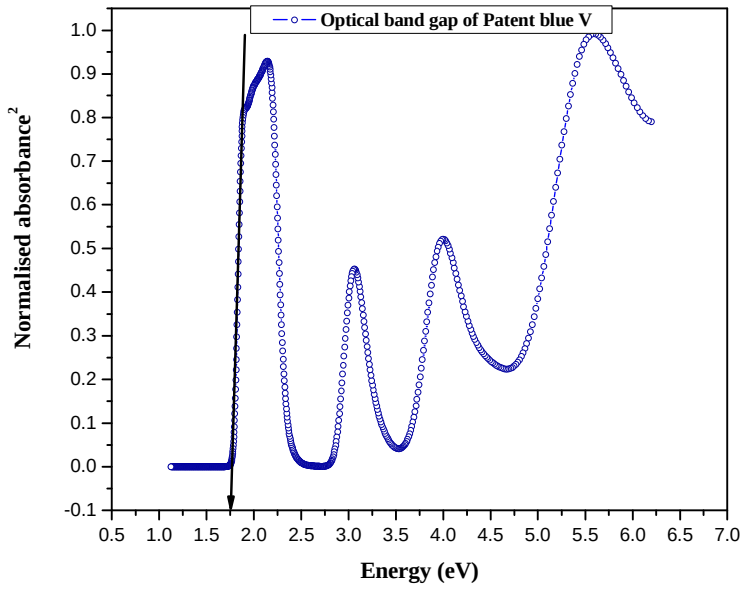

Figure 3. Optical bad gap of patent blue V dye

Thermal properties

The TGA and DTA curve of patent blue V is represented in Fig. 4. TGA and DTA curves were obtained by heating 8.706 mg patent blue V from 35 to 500 ◦C at a heating rate of 10 ˚C/min in a flow rate of 150 ml min^{-1} using pure nitrogen atmosphere to avoid thermal oxidation. This change occurs when the sample looses or gains due to decomposition or reaction with the surrounding atmosphere and consequently produces steps in the TGA curve. TGA shows four steps of mass change with temperature. These four steps occurred at 35–75 ˚C, 75–150 ˚C, 150-215 ^{o}C and 285–412 ˚C, respectively. At first step (35–75 ˚C), the molar mass of the eliminated molecule can be

calculated. The molar mass of patent blue V is 582.66 g/mol; the mass loss is 9.84 % at 35–75 ˚C correspond to 57.33 g/mol. The most possibility in this step is evaporation of volatile constituents like water of crystallization or self humidity of patent blue and so H_2O with molar mass 18.1 g/mol is the most likely decomposition product. The change in mass 75 to 150 ^oC of temperature was found 12.37%. In the next step (i.e. 150–215 ˚C), there is a slighlity decrease in mass of patent blue V on heating shows good stability. The mass loss in this step was in 13.82 %. On further heating, 285-415 ^oC temperature fast degradation of patent blue V occurs with huge loss of mass 58.52%. This decrease in the mass ratio is due to decomposition of low molecular mass constituent (CH_3) with molar mass 15.04 g/mol and the decomposition of (SO_3Na) group with molar mass 103.1 g/mol which is responsible for the mass decrease in this range of temperature. Amorphous solids are known to exist in three physical states, the glassy, the rubber-like and the viscofluid states. The glassy state is characterized by vibration motion of the atoms constituting the compound chain about an equilibrium position. Therefore, the glass–glass transition peak at 65 ˚C, 132 ˚C, 212 ˚C, 302 ˚C, 318 ˚C and 340 ˚C may apparently be due to the motion of comparatively small kinetic (CH_3), (Na) and (SO_3) side groups. With increasing the temperature, there is a chance for the main chain to absorb more heat which helps in re-crystallizing of amorphous portions in a patent blue V. With further heating, the vibration motion of compound molecules increases. As a result, the material undergoes a viscofluid state. So that, the last peak at 303 ◦C is assigned as melting point of patent blue V and accompanied with decomposition of the molecule.

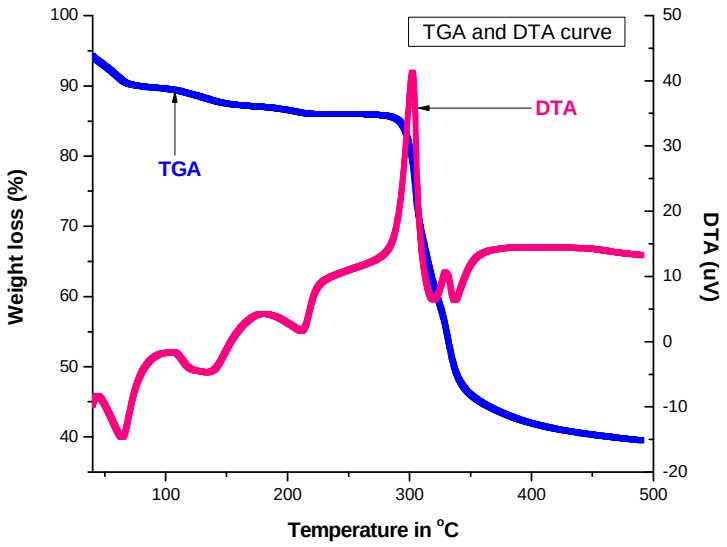

Figure 4. TGA and DTA plot of patent blue V dye

Photovoltaic properties

The performance of the dye as sensitizers for DSSCs were evaluated by short circuit current (J_{sc}), open circuit voltage (V_{oc}), fill factor (FF), and energy conversion efficiency (η). The parameters J_{sc} and V_{oc} of each cell were evaluated from its J–V curve. The overall performance of the above described solar cell can be evaluated in terms of cell efficiency (η) and fill factor (FF) expressed

$$FF = \frac{V_{max}.J_{max}}{V_{oc}.Jsc}$$

equ.----------(3)

$$\eta = \frac{V_{oc}.J_{sc}.FF}{P_{in}} \times 100$$

equ.----------(4)

where J_{sc} is the short-circuit current density ($mAcm^{-2}$), V_{oc} the open-circuit voltage(V),and P_{in} the incident light power. J_{max} and V_{max} correspond to current and voltage values, respectively, where the maximum power output is given in the J–V curve. In the band gap theory, the difference between the quasi-Fermi level of the TiO_2 layer and the electrolyte redox potential determines the maximum voltage generated under illumination. As shown in Eq.(5) the open-circuit voltage varies with the iodide concentration because there combination reaction occurs between the electrons on the conduction band of TiO_2 and I_3^- (triiodide) [21].

$$V_{oc} = \frac{kT}{q} \ln\left[\frac{\eta \phi_o}{n_o k_{et} [I_3^-]}\right] \quad \text{equ. ----------(5)}$$

where η is the quantum yield of photo generated electron for the given incident photo flux (ϕ_0); n_o represents the electron density on the conduction band of TiO_2 in the dark, while ket reflects the recombination reaction rate for the given triiodide concentration [I_3^-].

The effect of addition of different inorganic and organic iodides with iodine on the performance of DSSC was investigated. The concentration of the redox electrolytes were iodine (I_2) (0.01M), potassium iodide (KI) (0.1M), tetramethylquaternaryammonium iodide [$(CH_3)_4NI$] (0.1M), tetraethylquaternaryammonium iodide [$(CH_3\ CH_2)_4NI$] (0.1M), tetrapropylquaternaryammonium iodide [$(CH_3CH_2CH_2)_4NI$] (0.1M) in acetonitrile solvent.

The configurations used for the fabrication of DSSCs were as:
(i) FTO (substrate)/nanocrystalline TiO_2 (Photoanode)/ patent blue V(as sensitizer)/KI with I_2 (as electrolyte) /graphite (catalyst)/ FTO (substrate).
(ii) FTO (substrate)/nanocrystalline TiO_2 (Photoanode)/ patent blue V (as sensitizer)/$(CH_3)_4NI$ with I_2 (as electrolyte) /graphite (catalyst)/ FTO (substrate).
(iii) FTO (substrate)/nanocrystalline TiO_2 (Photoanode)/ patent blue V (as sensitizer)/ $(CH_3CH_2)_4NI$ with I_2 (as electrolyte) /graphite (catalyst)/ FTO (substrate).
(iv) FTO (substrate)/nanocrystalline TiO_2 (Photoanode)/ patent blue V (sensitizer)/$(CH_3CH_2CH_2)_4NI$ with I_2 (as electrolyte) /graphite (catalyst)/ FTO (substrate).

Current density-voltage characterization of DSSC based on patent blue V dye sensitizer is shown in figure 5. The photovoltaic parameters of the fabricated cells presented in Table 1. Open circuit voltage (V_{oc}) and short circuit current (J_{sc}) were obtained 0.393 V and 0.118 mA/cm^2 respectively with redox electrolyte KI-I_2 in acetonitrile solution (Table 1). Improvement of V_{oc} (0.412) was found with $(CH_3)_4NI$-I_2 redox electrolyte. However, lowest J_{sc} (0.091 mA/cm^2) was obtained with low efficiency (0.147) in $(CH_3)_4NI$-I_2 redox electrolyte. In $(CH_3CH_2)_4NI$-I_2 redox electrolyte, highest V_{oc} (0.434 V) was obtained and Jsc (0.115 mA/cm^2) were found with efficiency (0.228). V_{oc} (0.400) was found with $(CH_3CH_2CH_2)_4NI$-I_2 redox electrolyte. However, highest J_{sc} (0.219 mA/cm^2) was obtained with highest efficiency (0.476) in $(CH_3)_4NI$-I_2 redox electrolyte. The effect of electrolytes on V_{oc} and J_{sc} for a patent blue V dye sensitized nanocrystalline TiO_2 solar cell under light source. The V_{oc} of the DSSC in quaternary ammonium iodide-iodine redox electrolyte derived from the energy gap between the conduction band level of the TiO_2 and the I^-/I_3^- redox potential of alkyl cations. As a result of this, the conduction band of the TiO_2 shifted negatively from CH_3 to C_3H_7, leading to the increase of the V_{oc} and the vice-versa [22]. The overall conversion efficiency performance increases in the order: $(CH_3)_4NI$-I_2<$(CH_3CH_2)_4NI$-I_2 <KI-I_2<$(CH_3CH_2CH_2)_4NI$-I_2.

Table 1. Photovoltaic properties of patent blue V

Electrolyte	V_{oc} (in V)	Current density (J_{sc}) (mA/cm^2)	Fill factor (FF)	Efficiency (η)
KI-I_2	0.393	0.118	0.574	0.266
$(CH_3)_4NI$-I_2	0.412	0.091	0.391	0.147
$(CH_3CH_2)_4NI$-I_2	0.434	0.115	0.456	0.228
$(CH_3CH_2CH_2)_4NI$-I_2	0.400	0.219	0.543	0.476

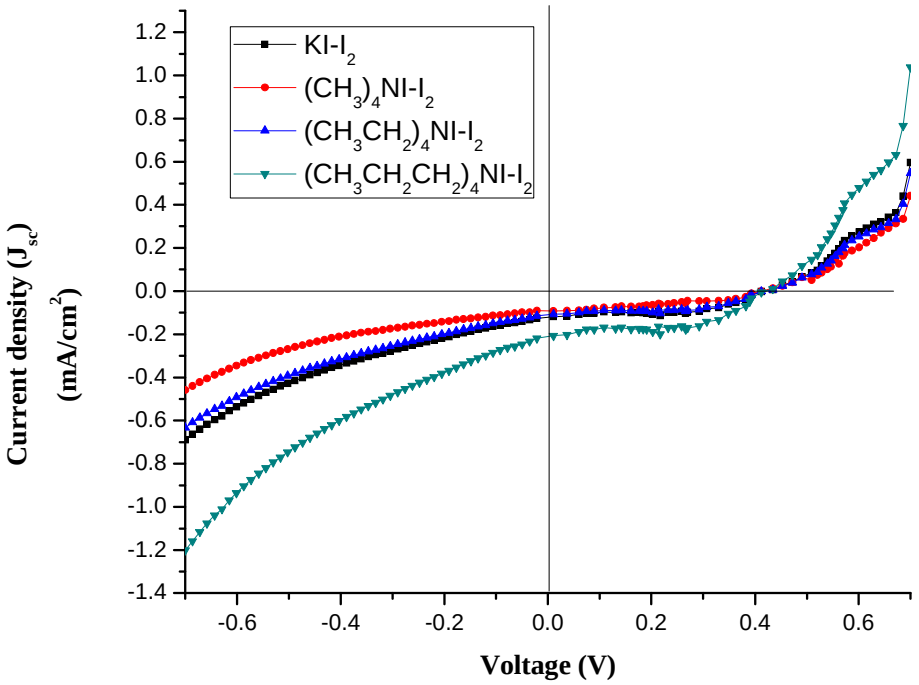

Figure 5. Current-voltage plot of fabricated solar cell with patent blue V dye

CONCLUSION

Dye sensitized solar cells were assembled using patent blue V dye as sensitizer and applying four redox electrolytes i.e. (KI), $[(CH_3)_4NI]$, $[(CH_3CH_2)_4NI]$ and $[(CH_3CH_2CH_2)_4NI]$, with iodine in acetonitrile solvent. Nano titania was used as semiconductor for fabrication of DSSC assembly with FTO glass substrate. Absorption spectra showed that the dye could be effectively applied as photosensitizers in DSSC. V_{oc} of fabricated solar cells was found in range of 0.393 to 0.434 V while J_{sc} was obtained in range 0.093 to 0.219 mA/cm^2. Maximum efficiency in these DSSCs (4.76) was found with $(CH_3CH_2CH_2)_4NI$-I_2 redox electrolyte. It was also analyzed that the efficiency of the dye sensitized solar cells can be enhanced by varying the redox electrolytes. The dye could be suitably used as effective sensitizers due to their electron injection process from the excited dye molecule to the conduction band of TiO_2 and hence the subsequent regeneration are feasible in these organic sensitized solar cells.

REFERENCES

[1]R.R. King, D.C. Law, K.M. Edmondson, C.M. Fetzer, G.S. Kinsey, H. Yoon, D.D. Krut, J.H. Hermer, R.A. Sherif, N.H. Karam, *Advances in Optoelectronics*, **2007** Article ID 29523. http://dx.doi.org/10.1155/2007/29523
[2] A. Goetzeger, C. Hebling C, *Solar Energy Material Solar Cells*, **2000**,62,1-19. DOI:10.1016/S0927-0248(99)00131-2
[3] B. Li, L. Wang, B. Kang, P. Wang, Y. Qiu, *Solar Energy Material Solar Cells*, 2006, 90, 549-573. DOI:10.1016/j.solmat.2005.04.039
[4]B. O'Regan, M. Gratzel, *Nature*, **1991,** 353, 737-740. DOI:10.1038/353737a0
[5]M. Gratzel, *Journal of Photochemistry and Photobiology A*,**2004**, 164, 3-14. DOI:10.1016/j.jphotochem.2004.02.023
[6] M.K. Nazeeruddin, C. Klein, P. Liska, M. Gratzel, *Coordination Chemistry Reviews*, **2005**, 249, 1460-1467. DOI:10.1016/j.ccr.2005.03.025
[7] T.A. Heimer, E.J. Heilweil, C.A. Bignozzi, G.J. Meyer, *J. Physical Chemistry A*, **2000,** 104, 4256-4262. DOI: 10.1021/jp993438y

[8]P.V. Kamat, M. Haria, S. Hotchandani, *J. Physical Chemistry B,* **2004,** 108, 5166-5170. DOI: 10.1021/jp0496699
[9]A. Furube, R. Katoh, T. Yoshihara, K. Hara, S. Murata, H. Arakawa, M. Tachiya, *J. Physical Chemistry B,* **2004,** 108, 12583-12593. DOI: 10.1021/jp0487713
[10] T. Dittrich, B. Neumann, H. Tributsch, *J. Physical Chemistry C,* **2007,** 111, 2265-2269.DOI: 10.1021/jp065830z
[11] X.Z. Liu, Y.H. Luo, H. Li, Y.Z. Fan, Z.X. Yu, Y. Lin, L.Q. Chen, Q.B. Meng, *Chemical Communication,* **2007,** 27, 2847-2849. DOI: 10.1039/B700472A
[12] J.B. Xia, F.Y. Li, H. Yang, X.H. Li, C.H.J. Huang, *J. Material Science*, **2007,** 42, 6412- 6416. DOI 10.1007/s10853-006-1184-3.
[13] K. Hara, T. Sato, R. Katoh, A. Furube, Y. Ohga, A. Shinpo, S. Suga, K. Sayama, H. Sugihara, H. Arakawa, *J. Physical Chemical B,* **2003,** 107, 597-606. DOI: 10.1021/jp026963x
[14]W. Xu, B. Peng, J. Chen, M. Liang, F. Cai, *J. Physical Chemical B,* **2008**, 112, 874-880. DOI: 10.1021/jp076992d
[15]Y. Xu, W.K. Chen, M.J. Cao, S.H. Liu, J.Q. Li, A.I. Philippopoulos, P. Falaras, *Chemical Physics,* **2006,** 330, 204-211. DOI:10.1016/j.chemphys.2006.08.012
[16]Y. Kurashige, T. Nakajima, S. Kurashige, K. Hirao, Y. Nishikitani, *J. Physical Chemistry A,* **2007,** 111, 5544-5548. DOI: 10.1021/jp0720688
[17] M.J. Lundqvist, M. Nisling, S. Lunell, B. Åkermark, P. Persson, *J. Physical Chemistry B,* **2006,** 110, 20513-20525. DOI: 10.1021/jp064045j
[18] Z.Y. Guo, Y. Zhao, W.Z. Liang, G.H. Chen, *J. Physical Chemistry C,* **2008,** 112, 16655- 16662. DOI: 10.1021/jp802007h
[19] N. Robertson, *Angewandte Chemie International Edition,* **2006,** 45, 2338-2345. DOI: 10.1002/anie.200503083
[20] J. Tauc, in: F. Abeles (Ed.), *The Optical Properties of Solids*, vol. 37, North-Holland, Amsterdam, **1972.**
[21] LanZ, Wu J, Wang D, Hao S, Lin J, Huang Y. *Solar Energy*, **2007,** 81(1), 117–122. DOI:10.1016/j.solener.2006.05.003
[22] K. Hara, T. Horiguchi, T. Kinoshita, K. Sayama, H. Arakawa, *Solar Energy Material Solar Cells*, **2001,** 70, 151-161.DOI:10.1016/S0927-0248(01)00019-8